Pion Decay and Nuclear Line Emissions from the 1991 June 11 Flare

Natalie Mandzhavidze[1,2], Reuven Ramaty[1], David L. Bertsch[1] and Edward J. Schneid[3]

[1]*Laboratory for High Energy Astrophysics, Goddard Space Flight Center, Greenbelt MD 20771*
[2]*Universities Space Research Association*
[3]*Northrop Grumman, Bethpage, NY 11714*

We reexamined the issue of continuous acceleration vs. trapping in the 1991 June 11 flare using a much broader data set than was available previously. We consider updated EGRET spark chamber data, high energy continuum and nuclear line data from EGRET/TASC, and 2.22 MeV line data from COMPTEL covering an extended time period. We find that the data indicate the existence of at least three distinct emission phases characterized by changes in the ion spectrum during transitions from phase to phase. By combining the 2.22 MeV and 4.44 MeV line fluxes with the pion decay emission flux in the first two phases, we show that ion spectrum hardened during the transition from the first to the second phase. We derive the ion spectrum in the third phase from a detailed spectral analysis of the EGRET spark chamber data and show that this spectrum is consistent with the 2.22 MeV line-to-pion decay flux ratio in this phase. The ion spectrum in the third phase is softer than that in the second phase. Concerning variability within the phases, we find that the ion spectrum probably remained constant during the second and third phases. This implies that the hitherto developed ion transport models are not appropriate for explaining the extended emission observed from the June 11 flare. We discuss a different scenario in which the ions are trapped in the low density coronal portions of loops but produce the gamma rays in the denser subcoronal interaction regions; this model of episodal acceleration and subsequent trapping could be consistent with the data.

I. INTRODUCTION

Gamma ray observations from several X-class flares in June 1991 provided evidence for the interaction of high energy ions in the solar atmosphere for long periods of time. The most striking example is the June 11 flare from which 50 MeV to 2 GeV gamma rays were observed with the EGRET spark chamber on the Compton Gamma Ray Observatory (CGRO) for 8 hours after the impulsive phase of the flare (1). Gamma rays up to GeV energies were also observed for about 2 hours with GAMMA-1 from the June 15 flare (2,3).

Such high energy gamma ray emission is most likely pion decay radiation produced by ions of energies up to several GeV interacting with the ambient solar atmosphere. The ions could either be accelerated in the impulsive phase and subsequently trapped at the Sun, be accelerated continuously over the duration of the emission, or be accelerated episodically and subsequently trapped between the acceleration episodes.

We have previously developed a transport model for high energy ions in solar flare loops which allowed us to calculate the time dependence, energy spectrum and angular distribution of the pion decay radiation produced by accelerated ions injected impulsively at the top of the loop (4). We then applied this model to the EGRET spark chamber observations of the June 11 flare and showed that the nuclear line emission, which is expected to accompany the high energy photons, should decay faster than the pion decay emission (5). On the basis of subsequent observations of nuclear lines (6–8), which provided some indication that the pion decay and 2.22 MeV line emissions had similar time profiles, we concluded that at least during the first 3 hours of the June 11 flare, pure trapping cannot account for the observations (9). An argument against trapping, based on the similarity of the combined pion decay–nuclear line time profile and microwave time profiles, was also presented for the June 15 flare (3,10).

In the present paper we reexamine this conclusion using new 2.22 MeV and 4.44 MeV nuclear line data and 150–210 MeV continuum data from EGRET/TASC (11), and 2.22 MeV line data from COMPTEL on CGRO (12). These data, together with microwave data (13) provide a much more detailed description of the time profiles of the various gamma ray emissions than was hitherto available. In particular, interpreting the 150–210 MeV continuum emission as pion decay emission, we are able to consider the time profile of the pion decay emission for the entire 8 hours starting from the impulsive phase of the flare; the EGRET spark chamber could not observe the impulsive phase because of the saturation of its anticoincidence dome. We present these data in §2. We find that the data indicate the existence of at least three distinct emission phases characterized by changes in the ion spectrum during transitions from phase to phase, with the spectrum probably remaining constant during the second and third phases. In §3 we determine power law spectral indexes for the ions in the three phases using 2.22 MeV and 4.44 MeV line, and pion decay flux ratios. We also carry out a full spectral analysis of the gamma rays observed with the EGRET spark chamber during a portion of the third phase. In this analysis, in addition to power laws we also consider the ion spectrum predicted by shock acceleration (14) with the spectral index which provides the best fit to the ground based neutron monitor observations of the interplanetary charged particles (GLE) from the June 11 flare (15). For simplicity, we carry out the calculations in an isotropic thick target model using various abundances for the accelerated particles [see (16,17) for more details]. In §4 we use the results to reexamine the issue of trapping vs. continuous acceleration and show that modifications to our

transport model would allow the long term trapping of ions in the second and third phases.

II. DATA

We present the various gamma ray fluxes in Fig. 1 together with the 17 GHz flux density (13).

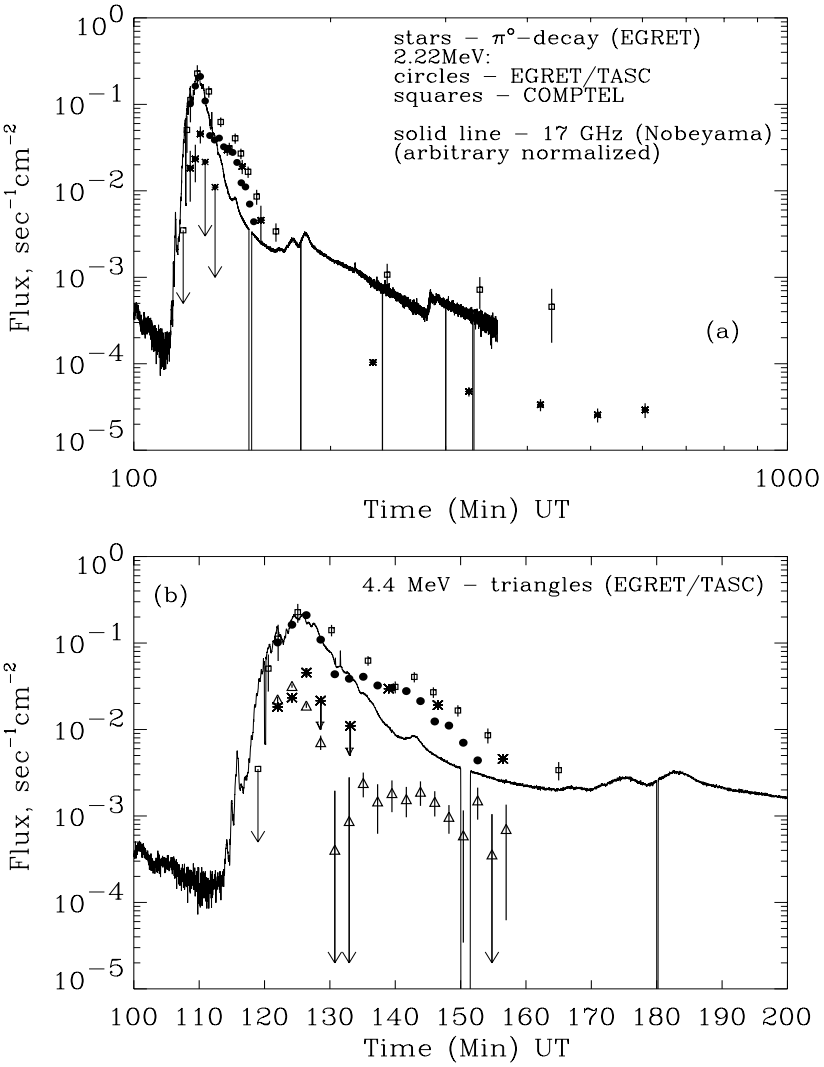

Fig. 1. Time dependence of the various emissions during the 1991 June 11 flare. The notation of panel (a) also refers to panel (b).

Panel (a) shows the data on an extended time scale covering 6 consecutive

CGRO orbits, while panel (b) shows the data on a more expanded time scale for only the first orbit. The closed circles and triangles represent, respectively, the 2.22 MeV and 4.44 MeV line fluxes observed with EGRET/TASC [see (11) for more details]. The open squares represent the 2.22 MeV line flux observed with COMPTEL (12). The 2.22 MeV COMPTEL data extend to much later times than do the 2.22 MeV EGRET/TASC data (Fig. 1a); during the first orbit (Fig. 1b), when the two data sets overlap, there is agreement between the fluxes at some times but differences as large as a factor of 2 can also be seen.

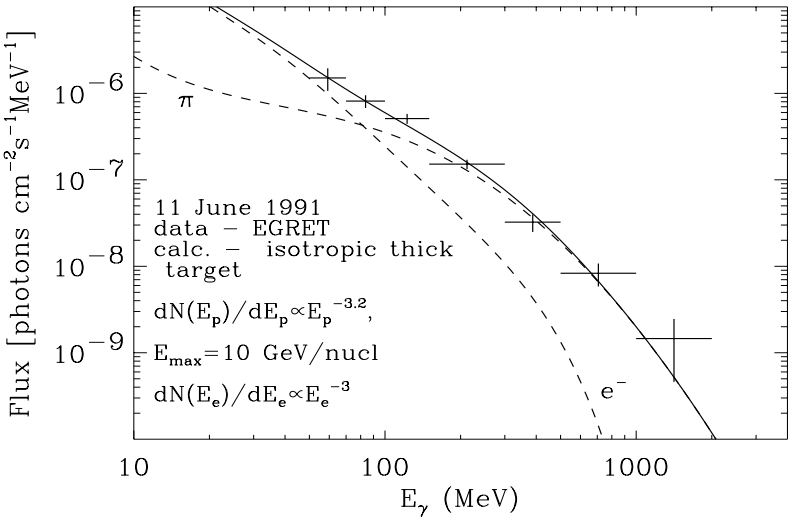

Fig. 2. Gamma ray spectrum during the 3.5 to 6 hour UT period on June 11 measured with the EGRET spark chamber. The calculated spectra are the best fitting combination of bremsstrahlung and pion decay emission.

The stars represent our estimated total π^o decay gamma ray fluxes. During the first orbit we based our estimate on the 150–210 MeV fluxes observed with EGRET/TASC. We assumed that all the observed counts in this highest energy channel are due to photons from π^o decay. Our calculations show that the ratio of the total π^o decay gamma ray flux to the 150–210 MeV flux is practically independent of the assumed particle energy spectrum and is equal to $\approx$6.3. There is practically no contribution from secondary $e^{\pm}$ bremsstrahlung and annihilation in flight in this channel. There might be, however, contributions from neutrons and primary electron bremsstrahlung. We have calculated the neutron flux that is expected to accompany the observed gamma ray emissions and found that the predicted time profile is quite different from the 150–210 MeV EGRET/TASC time profile; in particular the neutron emission peaks at about 130 min UT, a time at which the 150–210 MeV EGRET/TASC flux is minimal, showing only upper limits (Fig. 1b). We thus believe that the contribution to the 150–210 MeV EGRET/TASC

data from neutrons is not very significant. On the other hand, to estimate the contribution of the primary electron bremsstrahlung a full spectral analysis of the EGRET/TASC data is required which is beyond the scope of this paper. However, by using the highest energy channel we have minimized this contribution.

During the next 5 orbits the π^o decay gamma ray flux is based on a new analysis of the EGRET spark chamber data (11). Using the results of this analysis we fitted the 50–2000 MeV gamma ray spectrum observed from 3.5 to 6 hours UT (second and third orbits) with theoretical spectra which include both pion decay radiation and primary electron bremsstrahlung. In Fig. 2 we show the calculated spectra which provide the best fit to these data. The calculations were performed using an isotropic thick target model and assuming power law energy spectra for the accelerated particles with various ion and electron spectral indexes. The spectra shown in the figure correspond to the indexes which minimize χ^2. This fitting allows us to determine the total π^o decay gamma ray emission which is the quantity plotted in Fig. 1a. As there is no evidence for the variability of the observed gamma ray spectrum over the entire period out to the sixth orbit (11), we used the same 50–2000 MeV to total π^o decay gamma ray flux ratio for orbits 4, 5, and 6 as that calculated for the 3.5 to 6 hour UT period.

III. ANALYSIS

Considering the fluxes shown in Fig. 1, we can distinguish three major emission phases. The first and second phases are separated by a transition at about 130 min UT when both the 4.44 MeV line and pion decay emission show only upper limits (Fig. 1b). The 2.22 MeV line is still detectable during this time because of its delayed nature. The onset of a 'bump' in the 2.22 MeV line flux is another indication of this transition. The transition between the second and third phases occurs around 170 min UT. The evidence for the third phase is provided by: (i) the change of slope in the time profiles of the 2.22 MeV line, pion decay and 17 GHz microwave data; (ii) the two peaks in the microwave data at 175 and 182 min UT indicating additional particle acceleration which may have started already at 165 min UT.

During the first phase the 2.22 MeV line flux exceeds the pion decay flux, while in the second phase these two emissions have almost equal fluxes (compare the closed circles and open squares with the stars before and after 130 min UT in Fig. 1b). This immediately implies that the ion spectrum is harder during the second phase than during the first phase. These two phases, however, are not manifest in the microwave emission, for which the 'bump' between 130 and 150 min UT seen in the nuclear emissions is absent (Fig. 1b). In the third phase the pion decay flux is again lower than the 2.22 MeV line flux, indicating a softening of the spectrum.

In Fig. 3 we compare the 2.22-to-4.44 MeV line fluence ratio calculated for

various power law spectral indexes s with the data for the two phases. As this ratio is strongly dependent on the accelerated α particle to proton ratio (17), we show calculations for three values of α/p. The range from about 0.01 to 0.5 is consistent with the broad variability of α/p seen in solar flare accelerated particle data (18). For the composition of the accelerated particles we used the same impulsive flare composition as used in our previous paper (17). The composition of the accelerated particles from impulsive flares is enriched in ^{3}He and heavy ions relative to the particle composition from gradual flares (18). We found (16,17) that the enhanced neutron production due to these enrichments is needed to account for the SMM observations of narrow gamma ray lines (19). For the ambient medium we assumed that the composition is photospheric; as we have shown previously (17) the coronal composition (20) leads to very similar results. We used neutron-to-2.22 MeV photon conversion factors appropriate for ions moving at 89° to a downward radius vector (21); this angular distribution provides a good approximation to an isotropic ion distribution; 35° is the heliocentric angle of the 1991 June 11 flare.

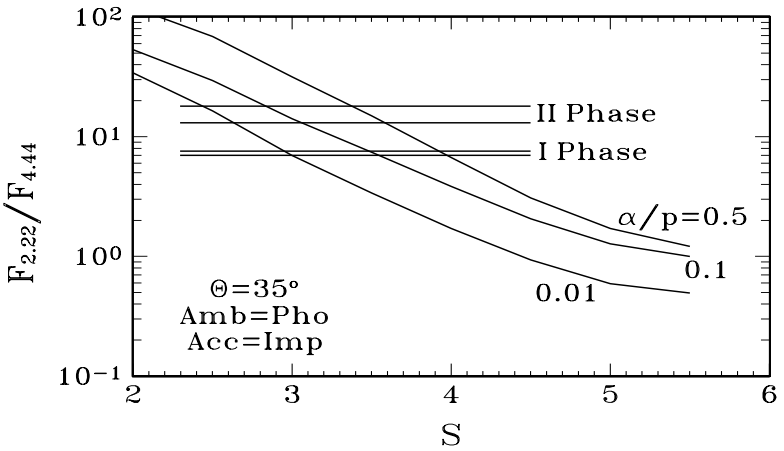

Fig. 3. 2.22 MeV-to-4.44 MeV line flux ratios. The horizontal lines are the measured (EGRET/TASC) ratios for the first and second phases; the calculated ratios are discussed in the text.

In Fig. 4 we show the π^o gamma ray to 4.44 MeV line fluence ratio. As we can see, this ratio is much less dependent on α/p. As opposed to the previous ratio, which probes the 10–100 MeV/nucl range, this ratio is sensitive to energies up to about a GeV. By comparing the calculations with the data we obtain $3.1 < s < 3.3$ for the first phase and $2.6 < s < 2.9$ for the second phase, showing that indeed the spectrum is harder in the second phase.

Considering the results of Fig. 3, we see that for the first phase the spectrum implied by $F(\gamma_\pi^\circ)/F_{4.44}$ is harder than the spectrum implied by $F_{2.22}/F_{4.44}$ for α/p=0.1 or 0.5, but softer than that implied by α/p=0.01. Since it is unlikely that the accelerated particle spectra flatten at high energies, either α/p is

less than 0.1 or there is a significant non-pionic contribution to the 150–210 MeV EGRET/TASC data. Such a contribution would lower $F(\gamma_\pi^\circ)/F_{4.44}$ and hence lead to a softer spectrum. On the other hand it is unlikely that α/p is as low as 0.01 since in our previous analysis (17) we found that this is not consistent with the narrow gamma ray line data from flares. For second phase, the spectrum implied by $F(\gamma_\pi^\circ)/F_{4.44}$ is consistent with that derived from $F_{2.22}/F_{4.44}$ for $\alpha/p \lesssim 0.1$, suggesting an unbroken power law spectrum from about 10 MeV to 1 GeV.

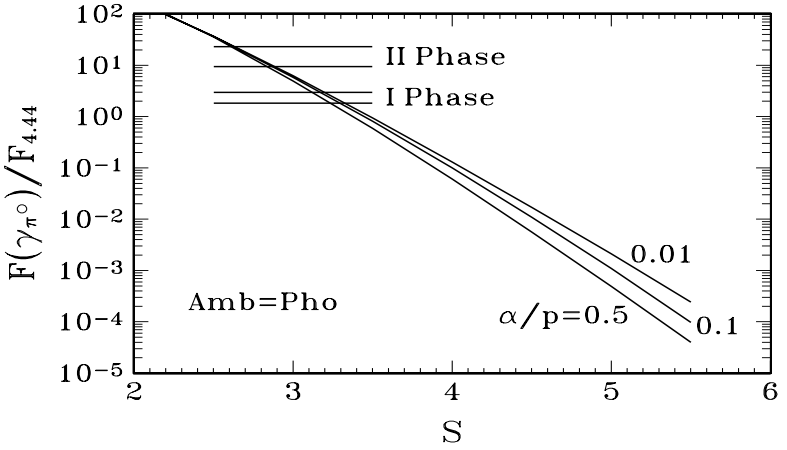

Fig. 4. π^o decay-to-4.44 MeV line flux ratios. The horizontal lines are the measured (EGRET/TASC) ratios for the first and second phases; the calculated ratios are discussed in the text.

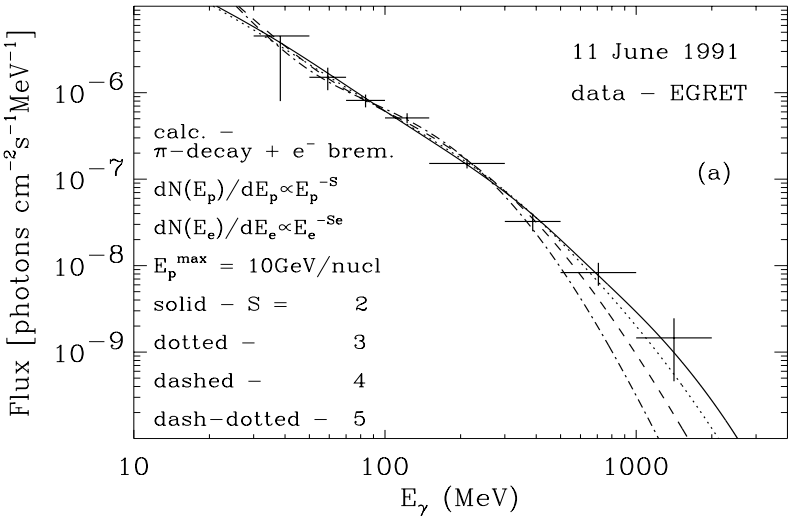

Fig. 5. Gamma ray spectrum during the 3.5 to 6 hour UT period on June 11. The curves show the effects of variations of the ion power law spectral index.

For the third phase, as already mentioned, we have carried out a full spectral analysis of the EGRET spark chamber data for the 3.5 to 6 hour UT period. The results are shown in Figs. 2, 5, 6 and 7. In Figs. 2, 5 and 6 we used power law ion spectra extending up to a high energy cutoff E_p^{max}. In Fig. 5 E_p^{max} is fixed at 10 GeV/nucl and the power law spectral index s is varied. For each s we select the primary electron spectral index s_e which provides the best fit to the data by minimizing χ^2. The overall best fit is provided by s=3.2 and s_e=3 for which the spectrum is shown in Fig. 2. For values of s greater than about 4 the calculated spectra become too steep at high energies. In Fig. 6 s is fixed and we varied E_p^{max}. We see that to account for the highest energy data point E_p^{max} has to be greater than about 8 GeV/nucl. While not shown in the figure, we found that increasing E_p^{max} above 10 GeV/nucl does not affect the calculated spectrum up to 2 GeV.

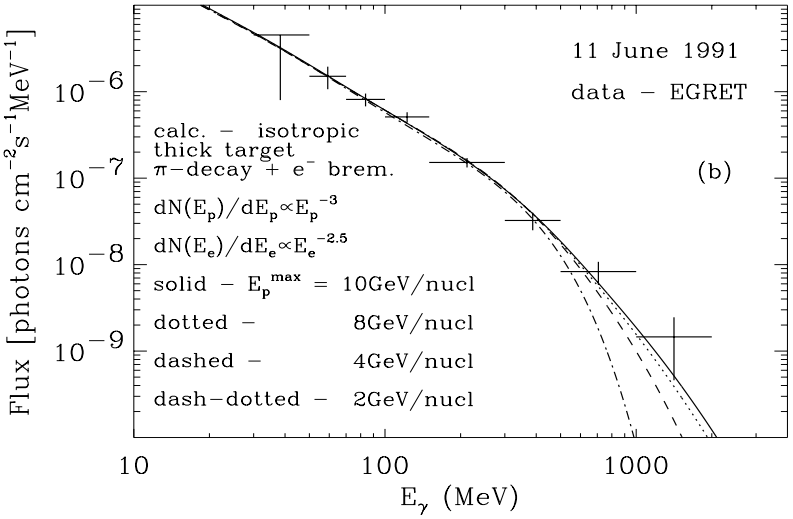

Fig. 6. Gamma ray spectrum during the 3.5 to 6 hour UT period on June 11. The curves show the effects of variations of the high energy cutoff.

In Fig. 7 we used the ion spectrum predicted by shock acceleration (14) with a spectral index which provides the best fit to the GLE observations of the June 11 flare (15). As before, we varied s_e to obtain the best fit for this ion spectrum. We set the high energy cutoff at 10 GeV/nucl. The GLE data seem to indicate a high energy cutoff at about 5 GeV/nucl (15). However, because of the steepness of the observed shock acceleration spectrum at high energies, the gamma ray spectra up to 2 GeV are practically identical for E_p^{max}=5 and 10 GeV/nucl. We see that calculated spectrum in Fig. 7 provides a reasonable fit to the data, except for the highest energy point. This may indicate that the spectrum of the interacting particles is harder than that of the interplanetary particles from the flare. This conclusion would be

even stronger if we compared the interplanetary particles with the interacting particles in phase two, since we found that the spectrum of the interacting particles during this phase was harder than that during phase three.

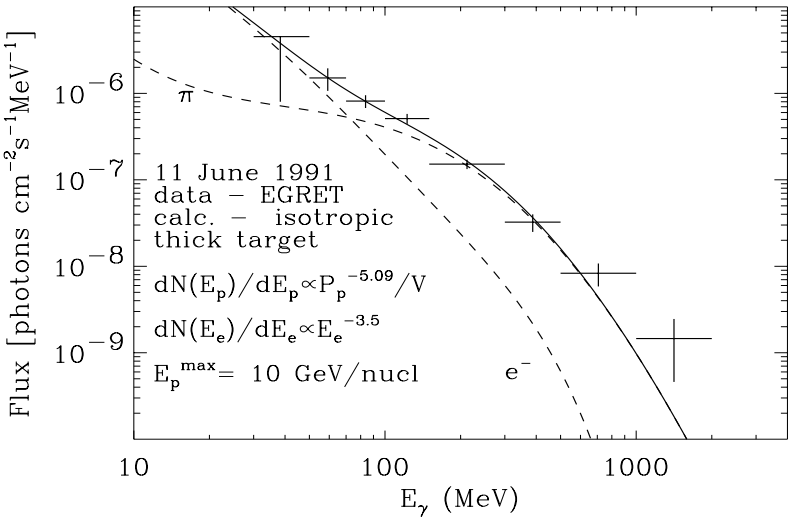

Fig. 7. Gamma ray spectrum during the 3.5 to 6 hour UT period on June 11. The calculations are for the shock acceleration spectrum which best fits the GLE observations of the June 11 flare (15).

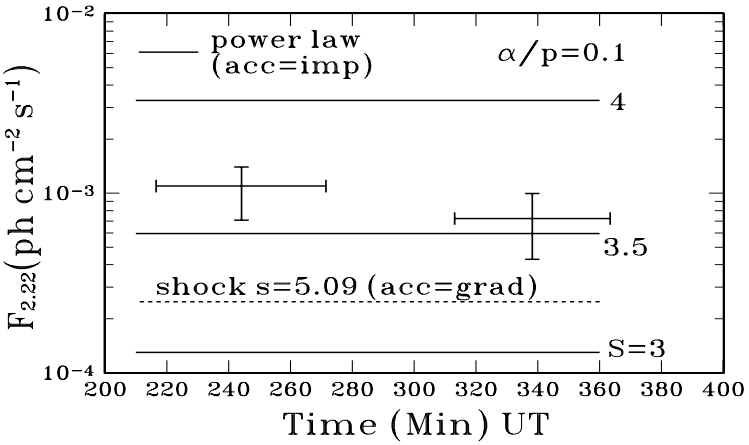

Fig. 8. 2.22 MeV line fluxes for the period 3.5–6 hours UT on June 11. Data points: COMPTEL (12); horizontal lines: average fluxes calculated by normalizing to the EGRET spark chamber data.

In Fig. 8 we compare the 2.22 MeV line flux observed with COMPTEL (12) with 2.22 MeV line fluxes obtained by normalizing the calculations to

the EGRET spark chamber data in the 3.5 to 6 hour UT interval. The solid lines are for power law ion spectra for which, as in Fig. 3, we used the impulsive flare composition for the accelerated particles. The dashed line is for the assumed shock acceleration spectrum. In this case we used the gradual flare composition because it is unlikely that shock acceleration will produce the impulsive flare enhancements of ^{3}He and heavy nuclei. For all the calculations in this figure we used the same neutron-to-2.22 MeV photon conversion factors as we did for the calculation in Fig. 3. We see that an ion spectrum with $s\sim3.5$ or slightly higher is consistent with the 2.22 MeV line flux. Such a spectrum is also consistent with the pion decay gamma ray spectrum (Fig. 5). The shock acceleration spectrum and a power law spectrum with s=3.2 (not shown in Fig. 8) underproduce the 2.22 MeV line flux. However, the following two effects can increase the 2.22 MeV-to-pion decay flux ratio: (i) an increase of α/p above the assumed value of 0.1 at least at low energies; (ii) an ion angular distribution pointing preferentially towards the photosphere which will enhance the neutron-to-2.22 MeV photon conversion and at the same time decrease the number of pion decay photons moving towards the observer. On the other hand, the assumption of the gradual flare composition for the accelerated particles in the case of the power laws would have decreased the calculated 2.22 MeV line flux; this could lead to a discrepancy between the ion spectrum determined from the spectral analysis and the 2.22 MeV line-to-pion decay emission flux ratio.

IV. DISCUSSION AND CONCLUSIONS

Considering the available data and calculations, it is clear that there were three major acceleration episodes in the June 11 flare giving rise to the interacting particles in the three phases that we have identified. The ion energy spectra in the three phases are different. The spectrum in the second phase is flatter than that in both the first and third phases. The data in the first phase do not allow us to study the possible variability of the spectrum within this phase. However, during the second and third phases the fact that the 2.22 MeV line-to-pion decay flux ratio is practically constant suggests that the spectrum within each phase does not vary with time. This is in conflict with the prediction of trapping models in which the particles are removed from the trap due to Coulomb and nuclear interactions in the trapping volume itself. Such models predict that the ion spectrum should harden with time leading to a faster decay of the 2.22 MeV line flux relative to the pion decay flux.

The loop model that we developed previously (4) made the same prediction. The model consisted of a coronal part in which both the magnitude of the magnetic field and the gas density were constant and two subcoronal portions in which the magnetic field and ambient gas density increased with increasing depth towards the photosphere. We took into account the magnetic mirroring of the ions in the subcoronal portions (but not in the coronal portion where

the field magnitude was constant), their pitch angle scattering due to plasma turbulence in the coronal portion, and their energy loss and removal due to Coulomb and nuclear interactions throughout the loop. Particles injected at the top of the loop were trapped between mirror points in the subcoronal regions, which, depending on the initial particle pitch angle, could lie fairly deep in the atmosphere. Thus, except for particles with pitch angles in the loss cones, the trapped particles interacted in the trapping volume causing the hardening of the ion spectrum with time and the faster decay of the 2.22 MeV line.

On the other hand if there is a strong convergence of the magnetic field lines also in the coronal portions of the loops, particles could be stored in a region of sufficiently low density, so that their spectrum remains constant in time. To trap protons of energies greater than 30 MeV for 5 hours (the duration of the observed overlap of the 2.22 MeV and pion decay fluxes in the third phase), the density in the trapping volume must be lower than 10^9 cm^{-3}. This value is reasonable for the coronal portion of moderately large loops. The gamma rays in this case will not be produced in the trapping volume; they will be produced after the precipitation of the ions into the subcoronal interaction regions. The trapping region will thus provide to the interaction region a source of particles with spectrum which remains constant in time, as required by the observed 2.22 MeV line and pion decay data. As the magnetic fields are expected to further converge in the subcoronal regions, the structure of the field and the depth profile of the ambient density must be such that all the precipitating particles, including those at the highest energies, will interact or lose their energy before they reach their mirror points in the interaction region. Otherwise, they will be reflected back into the trapping volume (with the reflection being more probable the higher particle energy) causing the energy spectrum of the trapped particles to flatten with time. However, if the particles interact before they reach their mirror points, their angular distribution will be forward peaked along the magnetic field lines. If the magnetic field is normal to the photosphere, as was assumed in the previous ion transport models (4,5,22), the pion decay radiation from flares near disk center (e.g. the June 11 flare) will show a strong cutoff at high energies due to the forward beaming of the emitted radiation (23). As this cutoff is in conflict with the EGRET spark chamber data [see fig. 10 of ref. (23)], our proposed model must further assume that there is a broad distribution of the magnetic field directions relative to the normal to the photosphere. Detailed calculations of gamma ray production in such models have not yet been carried out.

The available data for the June 11 flare may thus be consistent with particle trapping between episodes of acceleration. The scenario that we proposed will naturally lead to interacting particles with a constant spectrum. On the other hand, it is questionable whether continuous acceleration can produce particles with a time independent spectrum over hours. Furthermore, the argument based on the similarity of the gamma ray and microwave time profiles in favor

of continuous acceleration for the June 15 flare (3,10) would not hold for the June 11 flare for which the microwave time profile and the gamma ray time profiles are quite different (Fig. 1).

We wish to acknowledge Paul Evenson for discussions on the trapping scenario outlined above.

REFERENCES

1. G. Kanbach et al., A&A (Suppl.) **97**, 349 (1993).
2. V. V. Akimov et al., 22nd Internat. Cosmic Ray Conf. Papers **3**, 73 (1991).
3. V. V. Akimov et al., 1993, 23rd Internat. Cosmic Ray Conf. Papers **3**, 111 (1993).
4. N. Mandzhavidze and R. Ramaty, ApJ **389**, 739 (1992).
5. N. Mandzhavidze and R. Ramaty, ApJ **396**, L111 (1992).
6. J. Ryan et al., in Compton Gamma Ray Observatory (AIP: NY) 631 (1993).
7. R. J. Murphy et al., in Compton Gamma Ray Observatory (AIP: NY) 619 (1993).
8. E. J. Schneid, AAS Winter Meeting, Crystal City, Virginia (1994).
9. R. Ramaty and N. Mandzhavidze, in Proc. of the Kofu Symp., eds. S. Enome and T. Hirayama, Nobeyama Radio Observatory Rept. No. 360, 275 (1994).
10. G. E. Kocharov et al., 23rd Internat. Cosmic Ray Conf. Papers **3**, 107 (1993).
11. D. L. Bertsch et al., ApJ, in preparation (1996).
12. G. Rank et al., this volume (1996).
13. S. Enome & H. Nakajima, private communication (1993).
14. D. C. Ellison & R. Ramaty, ApJ **298**, 400 (1985).
15. D. F. Smart and M. A. Shea, this volume.
16. R. Ramaty, N. Mandzhavidze, B. Kozlovsky, and R. J. Murphy, ApJ, **455**, L193 (1995).
17. R. Ramaty, N. Mandzhavidze, and B. Kozlovsky, this volume.
18. D. V. Reames, J-P. Meyer, and T. T. von Rosenvinge, ApJ (Suppl.) **90**, 649 (1994).
19. G. H. Share and R. J. Murphy, ApJ **452**, 933 (1995).
20. D. V. Reames, Adv. Space Res. **15**, (7) 41 (1995).
21. X.-M. Hua and R. E. Lingenfelter, Solar Phys. **107**, 351 (1987).
22. X.-M. Hua, R. Ramaty, and R. E. Lingenfelter, ApJ **341**, 516 (1989).
23. R. Ramaty & N. Mandzhavidze, in High Energy Solar Phenomena—A New Era of Spacecraft Measurements, (AIP: NY), 26 (1994).